Kinetic energy of protons in ice Ih and water: A path integral study

R. Ramírez[*] and C. P. Herrero

Instituto de Ciencia de Materiales de Madrid (ICMM), Consejo Superior de Investigaciones Científicas (CSIC),
Campus de Cantoblanco, E-28049 Madrid, Spain

The kinetic energy of H and O nuclei has been studied by path integral molecular-dynamics simulations of ice Ih and water at ambient pressure. The simulations were performed by using the q-TIP4P/F model, a point-charge empirical potential that includes molecular flexibility and anharmonicity in the OH stretch of the water molecule. Ice Ih was studied in a temperature range between 210 and 290 K, and water between 230 and 320 K. Simulations of an isolated water molecule were performed in the range 210–320 K to estimate the contribution of the intramolecular vibrational modes to the kinetic energy. Our results for the proton kinetic energy K_H in water and ice Ih show both agreement and discrepancies with different published data based on deep inelastic neutron-scattering experiments. Agreement is found for water at the experimental melting point and in the range 290–300 K. Discrepancies arise because data derived from the scattering experiments predict in water two maxima of K_H around 270 and 277 K, and that K_H is lower in ice than in water at 269 K. As a check of the validity of the employed water potential, we show that our simulations are consistent with other experimental thermodynamic properties related to K_H, such as the temperature dependence of the liquid density, the heat capacity of water and ice at constant pressure, and the isotopic shift in the melting temperature of ice upon isotopic substitution of either H or O atoms. Moreover, the temperature dependence of K_H predicted by the q-TIP4P/F model for ice Ih is found to be in good agreement with results of path integral simulations using *ab initio* density-functional theory.

I. INTRODUCTION

The kinetic energy of atomic nuclei in molecules and condensed phases in thermodynamic equilibrium is related to the interatomic potentials present in the system. Thus although in the classical limit the average kinetic energy of a nucleus does not depend on details of its environment and interatomic interactions, but only on the temperature (equipartition principle), in a quantum approach the kinetic energy of a nucleus gives information on the effective potential in which the particle moves.

Deep inelastic neutron scattering (DINS) has been recently applied to study the thermal average of the kinetic energy of protons, K_H, in water and ice. K_H is derived from the measured neutron-scattering function by data analysis that includes several numerical corrections, such as the subtraction of the cell signal,[1] the application of theoretical models as the impulse approximation (which considers that the neutrons are scattered by single atoms with conservation of momentum and kinetic energy of the neutron plus the target atom), and numerical procedures to perform an integral transform of the scattering function to obtain the momentum distribution of the target atom.[2] Therefore analysis of experimental DINS data is not free of numerical limitations that have led in the past to reinterpretation of results. For example, the effective potential of H along the stretching direction of the OH bond in supercritical water at 673 K was considered as a double well potential on the basis of DINS measurements,[3] however, later experiments with longer counting times and subtraction of the cell signal did not show any evidence for such double well potential.[4]

For water, DINS investigations have been performed at atmospheric pressure and various temperatures: 300,[4] 296,[3] 271,[5] and 269 K.[5] The last two temperatures correspond to supercooled water and a substantial increase in K_H of about 58% (at 271 K) and 40% (at 269 K) was reported with respect to ambient water. This large increase was heuristically interpreted to be a consequence of a double well potential felt by delocalized H atoms.[5,6] However, a controversy has arisen about the data analysis at these temperatures, and it has been claimed that the observed data can be also explained without invoking large changes in K_H and without assuming the delocalization of H in a double well potential.[7] Very recently a new set of DINS experiments have been performed for water at temperatures in the range 272–285 K, and seemingly what appears as a unique set of measurements have been published by two different groups.[8,9] From an analysis of their experimental data these authors found a maximum in K_H at about 277 K that was considered as an evidence of a new water structural anomaly related to the well-known existence of a maximum in the density of water at the same temperature.[8] DINS derived values of K_H have been also reported at 5 K and at 269 K for the stable phase of ice at atmospheric pressure (ice Ih).[3,10]

The calculation of K_H in ice Ih has been done so far with the help of empirical models consisting of a set of decoupled quantum harmonic oscillators whose frequency is derived from optical data and measured vibrational density of states. The contribution of each harmonic oscillator to K_H was determined by the average number of excited phonons at the given temperature and by an estimation of the H participation in each normal mode.[11] This numerical approach predicts that K_H in ice Ih is nearly constant between 5 and 300 K. Similar empirical calculations have been performed for water.[11] A limitation of such approaches is that they are based on experimental information and neither the pressure nor the density of the condensed phase can be explicitly considered in the model.

Momentum distributions of protons in ice and water have been derived by path integral (PI) simulations specially designed to sample nondiagonal density matrix elements. The first attempts used empirical water models to study ice at 269 K,[12,13] and supercritical water at 673 K.[13] Water molecules were treated later by *ab initio* density-functional theory (DFT) in studies of ice at 269 K and water at 300 K,[14] obtaining for the radial proton momentum distribution closer agreement to experiment. The thermal average of the proton kinetic energy K_H can be calculated from the width of its momentum distribution. However, K_H is more easily accessible in standard PI simulations that sample diagonal elements of the density matrix, by the calculation of the virial estimator of the kinetic energy.[15,16] PI simulations of the kinetic energy of atomic nuclei have shown good agreement with data derived from neutron-scattering experiments in solid neon.[17,18]

In the present paper the virial estimator of the kinetic energy K has been calculated for water and ice Ih at atmospheric pressure by PI simulations. The empirical q-TIP4FP/F model has been chosen for the water simulations because it is an anharmonic flexible potential that reproduces the experimental density-temperature curve of water at atmospheric pressure with reasonable accuracy.[19] This potential model has been recently employed to study the isotopic shift in the melting temperature of ice Ih.[20] The partition of the kinetic energy into H- and O-atom contributions (K_H, K_O) has allowed the comparison to data derived from DINS experiments. To assess the reliability of our simulations for K_H we discuss also several thermodynamic properties that depend on the kinetic energy, as the constant pressure heat capacity C_p of ice and water and isotopic shifts in the melting temperature of ice. An additional check of the employed potential model has been conducted by comparing the temperature dependence of K_H in ice Ih to results derived by PI simulations based on *ab initio* DFT calculations using the SIESTA method.[21,22]

The structure of this paper is as follows. In Sec. II a short summary of the employed computational conditions is presented. Then the results obtained with the q-TIP4P/F model for the thermal average of the kinetic energy of ice, water, and an isolated molecule are given and compared to available experimental data and also to *ab initio* DFT simulations. In Sec. III the simulation results of C_p at 271 K are presented for ice and water and compared to experiment. In Sec. IV it is shown that kinetic-energy differences between solid and liquid phases at isothermal conditions determine the sign of the isotopic shift in the melting temperature. Finally, we summarize our conclusions in Sec. V.

II. KINETIC ENERGY

A. Computational conditions

In the PI formulation of statistical mechanics the partition function is calculated through a discretization of the integral representing the density matrix. This discretization defines cyclic paths composed by a finite number L of steps, that in the numerical simulation translates into the appearance of L replicas (or beads) of each quantum particle. Then, the implementation of PI simulations relies on an isomorphism between the quantum system and a classical one, derived

from the former by replacing each quantum particle (here, atomic nucleus of H and O atoms) by a ring polymer of L classical particles, connected by harmonic springs with a temperature- and mass-dependent force constant. Details on this computational method are given elsewhere.[23–26] The configuration space of the classical isomorph can be sampled by a molecular-dynamics (MD) algorithm, which has the advantage against a Monte Carlo method of being more easily parallelizable, an important fact for efficient use of modern computer architectures. Effective reversible integrator algorithms to perform PIMD simulations have been described in detail in Refs. 27–30. Reference 31 introduces useful algorithms to treat full cell fluctuations and multiple time step integration. All calculations were done using originally developed software and parallelization was implemented by the MPI library.[32]

PIMD simulations in the isothermal-isobaric *NPT* ensemble (*N* being the number of particles, *P* the pressure, and *T* the temperature) were conducted for ice Ih and water by using the point-charge, flexible q-TIP4P/F model. This model was parametrized to provide the correct liquid structure, diffusion coefficients, and infrared absorption frequencies (including the translational and librational regions) in quantum simulations.[19] Water simulations were done on cubic cells containing 300 molecules, while ice simulations included 288 molecules in a proton disordered orthorhombic simulation cell with parameters $(4a, 3\sqrt{3}a, 3c)$, with (a,c) being the standard hexagonal lattice parameters of ice Ih. The total kinetic energy is defined as $K = 2K_H + K_O$. The kinetic energy of the H and O nuclei (K_H, K_O) were derived by the virial estimator.[15,16,29] We stress that K_H and K_O are obtained as expected averages using the exact quantum partition function of the q-TIP4P/F water model, i.e., our calculation of quantum kinetic energies is free of any other physical assumption apart from the statistical uncertainty inherent to the actual PIMD simulations and the use of an empirical potential model. Expected averages were derived in runs of 5×10^5 MD steps (MDSs) for water and 2.5×10^5 MDSs for ice Ih, using in both cases a time step of 0.3 fs. The presence of disorder and spatial density fluctuations in the liquid causes larger simulation runs to be required for water. The system equilibration was conducted in runs of 5×10^4 MDSs. To have a nearly constant precision in the PI results at different temperatures, the number of beads L was set as the integer number closest to fulfill the relation $LT = 6000$ K, i.e., at 210 K the number of beads was $L = 28$. Additional computational conditions are identical to those employed in Ref. 20 and they are not repeated here. The simulations were done at atmospheric pressure in a temperature range 210–290 K for ice Ih and 230–320 K for water.

Additionally the kinetic energy K_{intra} associated to the three vibrational modes of an isolated water molecule was obtained by PIMD simulations at temperatures between 210 and 320 K. In the case of an isolated molecule the virial estimator allows the calculation of the oxygen $K_{\text{O,intra}}$ and hydrogen $K_{\text{H,intra}}$ contributions to the vibrational energy K_{intra}. The six translational and rotational degrees of freedom of an isolated water molecule behave classically at the studied temperatures and their kinetic energy ($k_B T/2$ per degree of freedom) has to be summed to K_{intra} to obtain the total kinetic energy K of the molecule. If m_O and M are the masses of

the oxygen atom and the water molecule, then the fraction of translational kinetic energy corresponding to the oxygen atom is given by m_O/M. Analogously for a classical rotation around a given axis, the fraction of the kinetic energy corresponding to the O atom is given by I_O/I, where I_O and I are the moment of inertia of the O atom and the water molecule with respect to the rotation axis. This ratio has to be calculated for three principal axes of the molecule to obtain the partition of the rotational kinetic energy into O and H contributions.[33] The energy unit used throughout this work (kJ/mol) refers to a mole of either the molecule (H_2O) or atom (O or H) under consideration.

Finally, we have performed PIMD simulations in ice Ih by coupling our PIMD program to the SIESTA code,[21,22] in such a way that the potential energy, atomic forces, and stress tensor used in the *NPT* simulations are derived from *ab initio* DFT calculations. The present implementation allows us to study only small simulation cells that are not large enough for an appropriate description of the disorder in the liquid state. We expect to overcome this limitation in the future by allowing the simultaneous parallelization of both PI and electronic structure codes. DFT results were derived for a $2 \times 1 \times 1$ supercell of the standard hexagonal cell of ice Ih with the aim of comparison to the data obtained with the q-TIP4P/F model. The DFT calculations were done within the generalized-gradient approximation with the PBE functional.[34] Core electrons were replaced by norm conserving pseudopotentials[35] in their fully nonlocal representation.[36] In this study a double-ζ polarized basis set was used and a grid of 27 k points was employed for the sampling of the Brillouin zone of the solid. Integrals beyond two-body interactions are performed in a discretized real-space grid, its fitness determined by an energy cutoff of 100 Ry. Average properties were derived by PIMD simulations runs of 4×10^4 MDS using a time step of 0.5 fs. Classical MD simulations of water using the SIESTA code have been published in Refs. [37–39].

B. Total kinetic energy

The temperature dependence of K calculated for ice Ih, water, and an isolated molecule with the q-TIP4P/F model potential is represented in Fig. 1. We observe that at a given temperature K is always larger in ice Ih than in water. For a molecule K is the sum of global rotational and translational terms (which are classical contributions at the studied temperatures), and a vibrational term K_{intra}, corresponding to the two OH stretches and the HOH bending mode. In Fig. 1 the temperature dependence of the K_{intra} term has been also shown for the isolated molecule. While K in ice and water increases with temperature, the vibrational term K_{intra} of the molecule remains nearly constant. This fact indicates that the three intramolecular vibrational modes remain mainly in their ground state in the studied temperature range, while vibrational modes related to the H-bond network display some amount of thermal population of excited states.

The partition of K in ice Ih and water into intra- and intermolecular contributions (K_{intra} and K_{inter}) is of interest to quantify the effect of the presence of H bonds in this observable. The intramolecular term K_{intra} is attributed to the internal vibrational modes of the molecule, while the intermolecular one, K_{inter}, is related to the librational (rotational)
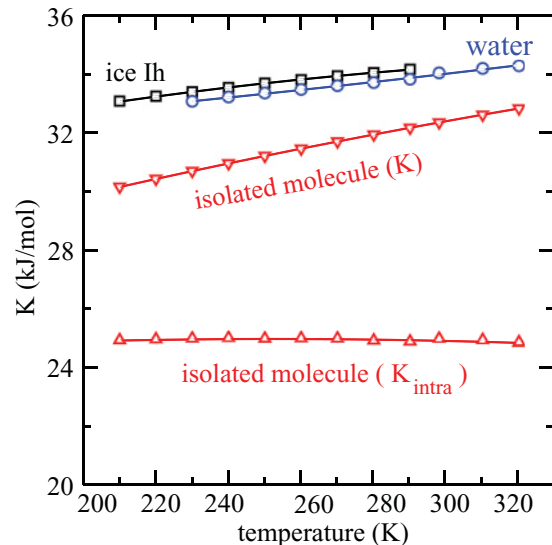

FIG. 1. (Color online) Thermal average of the kinetic energy of ice Ih and water as a function of temperature, as calculated by PIMD simulations with the q-TIP4P/F potential model at $P = 1$ atm. The kinetic energy K of an isolated molecule and its vibrational contribution K_{intra} are also given. The calculated error bars for ice and water are smaller than 0.01 kJ/mol and for the molecule amount to 0.05 kJ/mol.

and translational motions of the water molecules in the condensed phases. The presence of a H-bond network causes a large broadening of the internal vibrational modes of the water molecule and a shift in the frequencies of their peaks in the infrared absorption spectra.[19] This fact implies that both inter- and intramolecular motions are clearly coupled in the condensed phases of water. Therefore the partition of the total kinetic energy is presented here only as an approximation for didactic purposes in ice and water, and it is not intended to suggest that both types of degrees of freedom may be treated as separable variables.

We estimate K_{intra} in ice Ih and water with the help of a proportionality relation based on the fact that at the studied temperatures K_{intra} is close to the kinetic energy of the ground state associated with three intramolecular modes, $K_{GS,intra}$. Particularizing to the case of ice we have

$$\frac{K_{intra}(ice)}{K_{intra}(molecule)} \approx \frac{K_{GS,intra}(ice)}{K_{GS,intra}(molecule)}. \quad (1)$$

As a rough estimation of the ground-state kinetic energy $K_{GS,intra}$ in either ice, water, or an isolated molecule, we employ here a quasiharmonic approximation, so that a vibrational mode of wave number ω displays a kinetic energy of $\hbar\omega/4$ in its ground state. Thus $K_{GS,intra}$ will be approximated as

$$K_{GS,intra} \approx \frac{\hbar}{4}\left(2\omega_{OH}^{QA} + \omega_{HOH}\right). \quad (2)$$

The wave number ω_{OH}^{QA} is used here as an estimation of the average wave number of the two stretching modes (symmetric and asymmetric) of an isolated water molecule or the corresponding vibrational bands in the condensed phases. ω_{OH}^{QA} is determined from the equilibrium bond distance d_{OH} of either ice, water, or an isolated molecule, by calculating

TABLE I. Thermal average of the kinetic energy K of water and ice Ih at atmospheric pressure and of an isolated water molecule. The results were derived by PIMD simulations at 270 K. The energy K has been partitioned into O- and H-atom contributions (K_O, K_H). For water and ice the estimated intramolecular and intermolecular contributions to K, K_O, and K_H are also given. For a molecule the classical translational and rotational energy is given as K_{tr+rot}. This classical term has been partitioned into O and H components. d_{OH} is the thermal average of the intramolecular OH distance, and ω_{OH}^{QA} is the quasiharmonic stretching wave number calculated at the distance d_{OH}. The last column displays the theoretical results of Ref. [11] for ice Ih at 269 K. Kinetic energies are given in kJ/mol (to convert to meV multiply by a factor of 10.37). The standard error in the final digit is given in parentheses.

	Molecule	Water	Ice Ih	Ice Ih[11]
K	31.69(5)	33.59(1)	33.93(1)	33.38
K_{intra}	24.96(5) (79%)	23.5 (70%)	23.2 (68%)	
K_{inter}		10.1 (30%)	10.7 (32%)	
K_{tr+rot}	6.73 (21%)			
K_O	4.68(1)	5.04(1)	5.09(1)	5.01
$K_{O,intra}$	1.53(1) (33%)	1.4 (29%)	1.4 (27%)	
$K_{O,inter}$		3.6 (71%)	3.7 (73%)	
$K_{O,tr+rot}$	3.16 (67%)			
K_H	13.50(2)	14.28(1)	14.42(1)	14.18
$K_{H,intra}$	11.72(2) (87%)	11.0 (77%)	10.9 (76%)	11.2(79%)
$K_{H,inter}$		3.3 (23%)	3.5 (24%)	3.0(21%)
$K_{H,tr+rot}$	1.78 (13%)			
d_{OH} (Å)	0.957	0.978	0.982	
ω_{OH}^{QA} (cm^{-1})	3688	3424	3375	

the second derivative of the potential energy with respect to d_{OH}, and by considering the actual O and H masses.[20] The bending wave number is $\omega_{HOH} = 1600$ cm^{-1}. We recall that the bending potential is described by a simple harmonic term in the employed water model.[19] The ground-state assumption for K_{intra} in Eq. (1) is further justified by noting that the excitation energy corresponding to the vibrational mode of lowest frequency, $\hbar\omega_{HOH}$, is about seven times larger than the thermal energy $k_B T$ at the highest studied temperature (320 K), and thus the thermal population of excited vibrational modes, as given by a Bose-Einstein statistics,[33,40] results vanishingly small.

The partition of K into K_{intra} and K_{inter} contributions is presented in Table I at a temperature of 270 K. For water the intermolecular contribution K_{inter} is estimated to be 30% (10.1 kJ/mol) of K, while for ice Ih this contribution is slightly larger (32%, 10.7 kJ/mol), in agreement with the expectation that H bonds in ice are stronger than in water.[41] We display also the average OH bond distance d_{OH} and the corresponding quasiharmonic stretching wave number ω_{OH}^{QA}. The bond distance increases in the order molecule $\ll$ water $<$ ice. We note that x-ray Compton scattering studies of water and ice Ih have shown that the elongation of the OH bond in ice Ih is correlated to its stronger H-bond network,[42] in agreement to the simulation results for d_{OH} and K_{inter} shown in Table I. Our result of K in ice Ih displays a reasonable agreement to a previous calculation that is based on the use of experimental vibrational frequencies assuming a harmonic approximation (see the last column of Table I).[11]

C. Kinetic energy of O and H nuclei

The O nuclei contribution K_O to the kinetic energy is presented in Fig. 2. K_O in the condensed phases is significantly larger than its classical limit, i.e., quantum effects related to

the oxygen mass are relevant for its kinetic energy. At a given temperature K_O is slightly larger in ice Ih than in water (see also the K_O values of ice and water at 270 K in Table I).

The temperature dependence of K_H is presented in Fig. 3 for ice and water. The K_H contribution to the kinetic energy is substantially larger than the K_O term and it is also much larger than the classical limit, i.e., quantum effects related to their low atomic mass are very important for H atoms. At a given temperature K_H is always larger in ice Ih than in water.
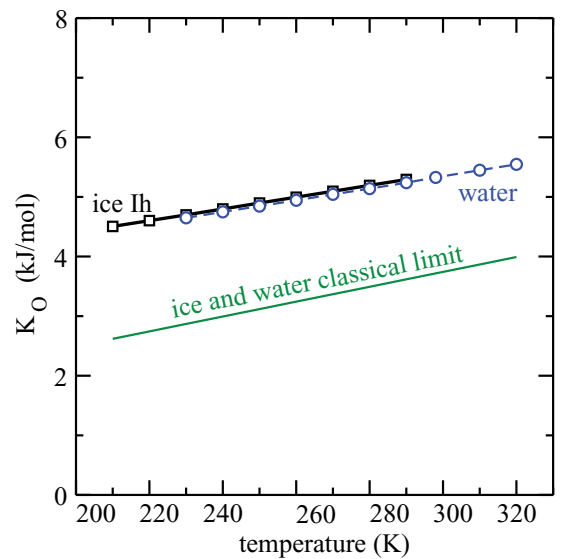

FIG. 2. (Color online) Oxygen contribution K_O to the kinetic energy of ice Ih and water as a function of temperature. The classical limit for ice and water amounts to $(3/2)k_B T$ per atom. The calculated error bars are smaller than 3×10^{-3} kJ/mol. For a given temperature, the difference of K_O in ice Ih and water ($\sim$0.05 kJ/mol) is significantly larger than the error bar.
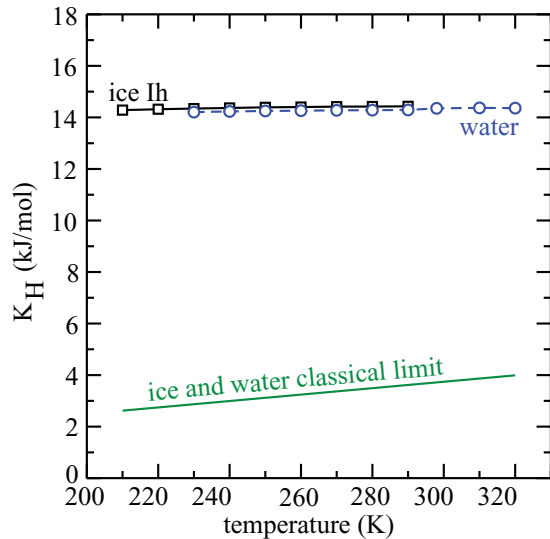
FIG. 3. (Color online) Proton contribution K_H to the kinetic energy of ice Ih and water as a function of temperature. The classical limit for the condensed phases corresponds to $(3/2)k_B T$ per atom. The calculated error bars are smaller than 5×10^{-3} kJ/mol. At constant temperature, the difference of K_H in ice Ih and water (~ 0.1 kJ/mol) is significantly larger than the error bar.

The partition of K_H and K_O into intramolecular and intermolecular contributions can be derived by assuming the following proportionality relation for the intramolecular kinetic energy in the condensed phases:

$$\frac{K_{H,intra}}{K_{O,intra}} \approx \left(\frac{K_{H,intra}}{K_{O,intra}} \right)_{molecule}, \qquad (3)$$

i.e., the ratio $K_{H,intra}/K_{O,intra}$ at a given temperature is assumed to be constant (~ 7.7) for ice, water, and an isolated molecule. Although we cannot provide a theoretical estimation of the error of this assumption, water molecules remain as clearly recognizable entities in the condensed phases at atmospheric pressure, and therefore the intermolecular interactions are not expected to change drastically the constant ratio assumed by Eq. (3). In Table I the result of this partition is given at 270 K. For water, the intermolecular contribution to K_O is larger than the intramolecular term (71% and 29%, respectively). However, in the case of K_H in water, the intermolecular contribution (23%, 3.3 kJ/mol) is much lower than the intramolecular term (77%, 11 kJ/mol, corresponding to the two OH stretches and the HOH bending mode). For ice Ih, having a stronger H-bond network than water,[41] we find that intermolecular contributions to K_O and K_H are slightly larger than in water, while the intramolecular contributions are slightly lower.

D. Comparison to DINS data

In Fig. 4 our K_H results are compared to data derived from DINS experiments.[3–5,8–10] Our calculation for water agrees reasonably well with the data derived from the neutron measurements at 273 K and the three values in the range 290–300 K. However, significant deviations are found in the temperature ranges between 269–272 K and 274–286 K.
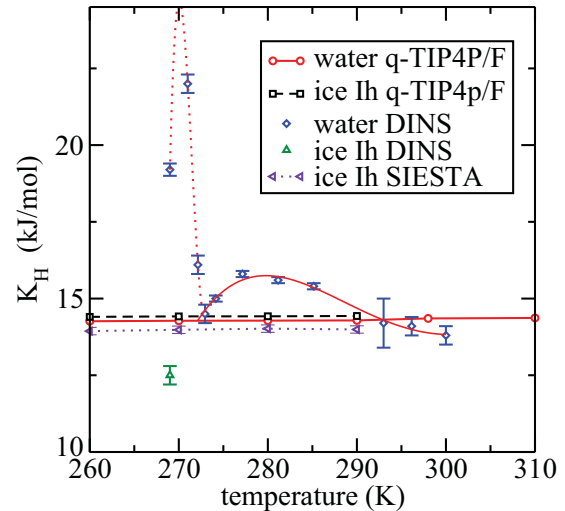

FIG. 4. (Color online) PIMD results obtained with the q-TIP4P/F model for the proton kinetic energy in water and ice Ih are compared to data derived from DINS experiments at temperatures in the range 269–300 K (Refs. [3–5,8–10]). Also PIMD results for ice Ih derived by *ab initio* DFT calculations with the SIESTA code are given. Lines are guides to the eyes.

The value of K_H derived at 271 K from the DINS experiment predicts an excess of 58% (8 kJ/mol) with respect to the room-temperature result. This excess was associated with a coherent delocalization of the proton between neighbor oxygen atoms.[8,9] However, this tentative explanation has been criticized by noting that measured proton momentum distribution implies a contracted proton wave function, which is inconsistent with the purported increased proton delocalization.[7] Moreover, coherent delocalization (i.e., tunneling) of a proton is associated with a resonance of the particle between two localized states. A coherent delocalization of the proton at $T_c = 271$ K would imply that the resonance frequency associated with the coherent process must be large enough to display the following relation to the thermal energy: $\hbar \omega_c \gg k_B T_c$. In other case the quantum coherence would be destroyed by thermal excitations. This inequality should remain valid if T_c increases to 273 K, i.e., a slight rise of 2 K should not provide enough thermal energy to destroy a coherent process of wave number ω_c for the proton. Therefore it seems somewhat contradictory that the excess of K_H attributed to a coherent process at 271 K disappears completely at 273 K.

An alternative explanation for the large value of K_H as a localized proton state at 271 K leads also to an unphysical picture. In this respect, as long as the water molecules maintain their molecular structure, i.e., without a dramatic increase in their stretching frequencies (which has been never observed), the intramolecular contribution to K_H must remain below the isolated molecule result of about 11 kJ/mol (see Fig. 3). Therefore an excess as large as 8 kJ/mol in the intramolecular energy seems to be incompatible with the experimental molecular structure of water.

The second maxima in K_H derived from the DINS experiments in the temperature range 274–286 K has been attributed to a new structural anomaly of water related to the existence of a maximum in the water density as a function of temperature.[8,9]
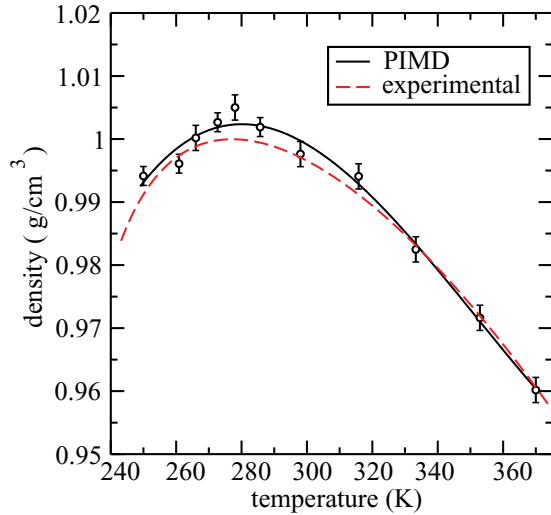
FIG. 5. (Color online) Density of water at 1 atm obtained from PIMD simulations and experimental data from Ref. 46. Simulation results correspond to runs of 4×10^6 MDS. The continuous line is a cubic fit to the simulation data.

This explanation is, however, not supported by our simulations. The employed water potential is able to reproduce realistically the experimental density maximum of water as a function of temperature (see Fig. 5).[19] In the temperature range between 274 and 286 K there appears a maximum in the density of water. Both experimental and simulation data agree in the fact that the water density in this temperature range changes by less than 1/1000. Our simulations predict that such a small density change does not affect K_H in any significant way (see Fig. 4). However, the excess in K_H at 277 K as derived from the DINS experiments amounts to 2.2 kJ/mol with respect to the room-temperature value. This excess energy is rather large, and of similar magnitude to the total H-bond network contribution to K_H that amounts to about 3.3 kJ/mol for the employed potential model (see Table I for our result of $K_{H,inter}$ in water at 270 K; this value remains nearly constant in the studied temperature range). Thus an excess of 2.2 kJ/mol represents, for the employed water model, an increase of 66% in the kinetic energy associated with the intermolecular interaction. We believe that such a large energetic modification should imply a dramatic change of the H-bond network that, however, has not been observed in any other spectroscopic or thermodynamical data of water around 277 K.

Another discrepancy between our simulations and the DINS analysis of K_H is that we find that at isothermal conditions K_H is about 0.14 kJ/mol larger in ice than in water. However, the DINS value reported for ice[10] at 269 K is much lower (~7 kJ/mol) than that of water[5] at the same temperature.

It is difficult to find a definite explanation for the agreement found between simulation data for K_H in water and those derived from neutron scattering at some temperatures (273 K and 290–300 K) and the discrepancies found at other temperatures (269–272 K and 274–286 K) and in the result for ice Ih. Both theoretical and experimental approaches include basic assumptions that might lead to unphysical results. From a theoretical side, the main limitation comes from the use of an empirical water potential. In particular, any dynamic process involving delocalization of protons between different molecules (i.e., breaking and forming of intramolecular OH bonds) cannot be described by the employed q-TIP4P/F potential. From the experimental side, the bibliography shows an experimental controversy concerning the validity of the models employed for the data analysis of the DINS experiments at 269 and 271 K.[6,7] Moreover, the numerical data analysis of the diffraction experiment implies corrections due to the experimental setup (detector position, subtraction of the cell signal) and a numerical integral transform that might be subject to numerical imprecisions. It has been mentioned in the Introduction that numerical reinterpretation of DINS experiments have already happened in recent times.[3,4]

In the face of this disagreement, the rest of the paper is intended as a consistency check for the ability of the employed empirical potential to reproduce the kinetic energy of the atoms in ice Ih and water. First, we go beyond the empirical potential by presenting results of *ab initio* DFT simulations.

E. Beyond the empirical potential

In Fig. 4 we show the K_H results for ice Ih derived from PIMD simulations using atomic forces calculated with the SIESTA code.[21,22] The temperature dependence of K_H predicted by the q-TIP4P/F model shows good agreement to the *ab initio* DFT results. The main difference between both sets of results is that values predicted by the q-TIP4P/F model are ~3% larger than the DFT ones. The origin of this shift is related to a different description of the OH stretching, as evidenced by a normal-mode analysis that provides harmonic stretching frequencies about 4% larger in the case of the q-TIP4P/F model. The *ab initio* data were derived in a small simulation cell (see Sec. II A). Thus the finite-size error has been estimated by comparing K_H values obtained in a small $(2a,a,c)$ and a large $(4a,3\sqrt{3}a,3c)$ supercell (i.e., containing 8 and 288 water molecules, respectively) by using the q-TIP4P/F model. This finite-size effect is rather low; the smaller cell shows a K_H value 0.3% lower than the larger one. We stress that the q-TIP4P/F potential was parametrized to give correct structure, diffusion coefficient, and infrared absorption frequencies in the *liquid state*.[19] Therefore the reasonable agreement to the *ab initio* data found for K_H in ice Ih should be considered as a realistic prediction of the empirical potential for a property that was not implicitly built in by the potential parametrization.

In the following sections we continue our check of the q-TIP4P/F potential by comparing some thermodynamical properties (heat capacity and isotopic shifts) that depend on the kinetic energy of the nuclei with experimental data.

III. HEAT CAPACITY AT 271 K

The enthalpy H calculated with the employed water model can be expressed as

$$H = V_{intra} + V_{inter} + K_O + K_H + PV, \quad (4)$$

where the first four summands give the internal energy as a sum of potential- (V) and kinetic-energy (K) terms and the potential energy is partitioned into a sum of intramolecular (V_{intra}) and intermolecular (V_{inter}) contributions. We have fitted our PIMD results for the enthalpy of ice and water to a quadratic function

TABLE II. Experimental results for C_p of water (Ref. 44) and ice Ih (Ref. 45) are compared with PIMD results at 271 K and 1 atm. The calculated C_p has been decomposed into potential- (C_{p1} and C_{p2}) and kinetic- (C_{p3} and C_{p4}) energy contributions. The numerical estimation of C_{p4} from the data derived from DINS experiments (Refs. 5, 8, and 9) is also given. The employed unit is J mol^{-1} K^{-1}.

	Water	Ice
C_p experimental	76.1	37.4
C_p PIMD	71.4 ± 2	36.1 ± 0.8
$C_{p1}(V_{\text{intra}})$	-9.0 ± 0.4	-7.4 ± 0.2
$C_{p2}(V_{\text{inter}})$	66.3 ± 1	31.6 ± 0.5
$C_{p3}(K_O)$	10.3 ± 0.2	9.9 ± 0.05
$C_{p4}(K_H)$	3.7 ± 0.2	2.0 ± 0.05
$C_{p4}(K_H, \text{DINS})$	-10^4	

of temperature in the range 250–290 K. Then the constant pressure heat capacity

$$C_p = \left(\frac{\partial H}{\partial T} \right)_P \qquad (5)$$

has been calculated at 271 K by performing the temperature derivative of the fitted function. The results are presented in Table II and compared to experimental data. The employed water model provides realistic values of C_p for both water and ice at 271 K. The deviation with respect to experiment amounts to about 6% in water and to 4% in ice Ih, with simulated values lower than experimental ones. Note that the experimental heat capacity of ice Ih is nearly one-half that of water, a fact that is reasonably reproduced by the simulations. This overall agreement encourages us to analyze separately the potential- (C_{p1}, C_{p2}) and kinetic- (C_{p3}, C_{p4}) energy contributions to C_p, as derived from the temperature derivative of the first four summands in Eq. (4). At atmospheric pressure the temperature derivative of the PV term gives a vanishingly small contribution to C_p.

The four contributions to the calculated C_p have been summarized in Table II. We note that the contribution C_{p1} of the intramolecular potential energy (V_{intra}) is negative for both water and ice Ih. This result is an anharmonic effect related to the reduction of the d_{OH} distance with increasing temperature, a fact that has been experimentally reported in water,[42,43] and that is reproduced by the employed model potential. The largest contribution (C_{p2}) to the heat capacity comes from the potential energy of the H-bond network, V_{inter}. C_{p2} amounts to 93% of the calculated C_p in water and to 88% in ice, a result in line with the expectation that the high heat capacity of water is a consequence of its H-bond network. Kinetic-energy contributions (C_{p3}, C_{p4}) are comparatively much lower. C_{p3}, derived from the temperature derivative of the kinetic energy K_O, is several times larger than C_{p4}, that is derived from K_H. In particular, we find that C_{p4} amounts to less than 4 J mol^{-1} K^{-1} (5% of the calculated C_p) in water.

The last line of Table II summarizes the value of C_{p4}, as derived from the temperature derivative of the K_H values obtained from the DINS experiments, that were plotted in Fig. 4. This contribution is negative and its absolute value

($\sim 10^4$ J mol^{-1} K^{-1}) is several orders of magnitude larger than the experimental heat capacity. Both sign and magnitude of this estimation of C_{p4} seem to be unphysical and incompatible with the experimental C_p data at 271 K. This fact led us to question if the maximum in K_H derived from the DINS analysis around 270 K (see Fig. 4) corresponds to any real physical effect.

IV. ISOTOPIC SHIFT IN THE MELTING TEMPERATURE

For ice Ih at atmospheric pressure experimental isotopic shifts indicate that heavier isotopes display higher melting temperatures. Thus deuterated ice Ih melts at a temperature 3.8 K higher than normal ice, while the isotopic shift for tritiated ice amounts to 4.5 K. Also H$_2$^{18}O melts at a temperature 0.3 K higher than ice Ih made of normal H$_2$^{16}O. Isotopic shifts in the melting temperature are a consequence of the dependence of the Gibbs free energy G on the isotope mass. At constant (T, P), this dependence results in a function of the kinetic energy of the isotope. Thus if G_H is the Gibbs free energy of a water phase containing ^{1}H atoms, the free energy of the corresponding deuterated phase, G_D, is given by the following relation:[20]

$$G_D = G_H - \int_{m_H}^{m_D} \frac{dm}{m} K_H(m), \qquad (6)$$

where m_H and m_D are the H and deuterium (D) masses, and $K_H(m)$ is the thermal average of the kinetic energy of a H isotope with mass m. Note that the mass m appears as an auxiliary variable in Eq. (6) and corresponds to a real isotope only at the integration limits (m_H, m_D). The Gibbs free-energy difference, $\Delta G = G_s - G_l$, between the solid (s) and liquid (l) phases at constant (T, P) can be expressed from Eq. (6) as

$$\Delta G_D = \Delta G_H - \int_{m_H}^{m_D} \frac{dm}{m} \Delta K_H(m), \qquad (7)$$

where

$$\Delta K_H(m) = K_{H,s}(m) - K_{H,l}(m). \qquad (8)$$

$K_{H,s}(m)$ is the isotope kinetic energy in the solid and $K_{H,l}(m)$ is the corresponding quantity in the liquid phase. A schematic representation of the free-energy difference ΔG_H at constant pressure is shown in Fig. 6 as a function of T. At the melting temperature T_H the free energy of both phases must be identical and ΔG_H vanishes. At temperatures below T_H we find that $\Delta G_H < 0$, i.e., the solid is the thermodynamically stable phase as it displays lower free energy than the liquid. However, for $T > T_H$ one finds $\Delta G_H > 0$ and then the stable phase is the liquid one. The isotope effect in the melting temperature can be obtained by calculating ΔG_D with the help of Eq. (7). A normal isotope effect implies that the definite integral in Eq. (7) takes a positive value. Thus at constant temperature ΔG_D becomes smaller than ΔG_H obtaining the schematic result represented in Fig. 6. Note that the melting point for the heavier isotope, T_D (where $\Delta G_D \equiv 0$), is shifted toward higher temperatures.

We conclude that it is the sign associated with the value of the definite integral in Eq. (7) that determines if the isotope effect in the melting temperature is normal (i.e., higher melting temperature for a heavier isotope mass if the sign is positive) or if it is an inverse isotope effect (lower melting point for a
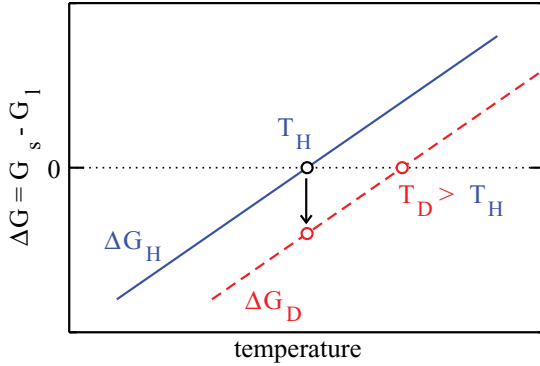
FIG. 6. (Color online) Schematic representation of the free-energy difference ΔG between solid and liquid phases of water as a function of temperature at constant pressure. The continuous line represents ΔG_H for phases containing the isotope ^{1}H and the melting temperature of the solid is T_H. Upon isotopic substitution of H by deuterium, the free-energy curve is shifted to the broken one, ΔG_D. At given temperature the shift of ΔG_D with respect to ΔG_H (shown by an arrow at the temperature T_H) can be calculated by the definite integral in Eq. (7). A normal isotopic shift implies that the melting temperature of the heavier isotope is higher ($T_D > T_H$).

heavier isotope mass if the sign is negative). A sufficient (but not necessary) condition to obtain a normal isotope effect is that

$$\Delta K_H(m) > 0; \quad \text{for } m_H \leqslant m \leqslant m_D, \quad (9)$$

i.e., the isotope kinetic energy is larger in the solid than in the liquid phase for the isotope masses m in the studied interval.

Our simulations show that the condition in Eq. (9) is satisfied for the isotopic substitution of H by either deuterium or tritium. The analogous condition, $\Delta K_O(m) > 0$, is also satisfied for the isotopic substitution of ^{16}O by ^{18}O, with $m(^{16}\text{O}) \leqslant m \leqslant m(^{18}\text{O})$. Thus the employed water model predicts normal isotopic shifts in the melting temperature upon isotopic substitution of either ^{1}H or ^{16}O by a heavier isotope, in agreement with experiment. Detailed results for deuterated and tritiated phases have been presented elsewhere.[20] The values collected in Table I at 270 K show that for hydrogen we get the value $\Delta K_H(m_H) = 0.14$ kJ/mol, i.e., K_H is larger in the solid than in the liquid, while for ^{16}O we find that K_O is 0.05 kJ/mol larger in ice than in water.

The K_H results derived from DINS data for water and ice Ih at 269 K give $\Delta K_H(m_H) = -6.7$ kJ/mol, i.e., K_H is much lower in ice than in water. Note that here the inequality of Eq. (9) is not satisfied for m_H. This fact implies that a small increase in the mass of hydrogen would produce an inverse isotope effect in the melting temperature. This behavior for m_H does not imply an inverse isotope effect for deuterium, because the latter effect is determined by the definite integral in Eq. (7), which involves all masses m with $m_H \leqslant m \leqslant m_D$. However, the value of $\Delta K_H(m_H) = -6.7$ kJ/mol at 269 K derived from the DINS analysis contrasts in sign and magnitude with our result of $\Delta K_H(m_H) = 0.14$ kJ/mol. We stress that the employed potential model provides a realistic prediction of the isotopic shift in the melting temperature of ice, a fact that let us expect that our calculation of $\Delta K_H(m_H)$ must be also

reasonably realistic.[20] This consideration raises further doubts about the physical significance of the maximum in K_H derived from the DINS analysis for liquid water around 270 K.

V. CONCLUSIONS

Quantum PIMD simulations at atmospheric pressure show that the q-TIP4P/F model provides realistic results for several thermodynamic properties of water and ice Ih. In particular, satisfactory agreement to experiment has been found in the dependence of the water density with temperature,[19] the isotopic shifts in the melting temperature of deuterated and tritiated ice,[20] and the constant-pressure heat capacity of water and ice Ih at 271 K. In the present paper we have focused on the calculation of the proton kinetic energy K_H and its comparison to available data derived from the analysis of neutron-scattering experiments,[3–5,8–10] and also to results based on *ab initio* DFT simulations.

This comparison has shown a remarkable agreement between the computational model and DINS data for water at some temperatures (273 K and in the range 290–300 K), but a strong disagreement at other similar temperatures (in the range 269–272 K and 274–286 K). Our simulations predict that K_H remains nearly constant in the temperature range where DINS data are available at atmospheric pressure. On the contrary, K_H values derived from the scattering experiments display a remarkable temperature dependence with two maxima at 270 and 277 K. This strong temperature dependence and, particularly, the large DINS value reported for K_H at 271 K (58% larger than at room temperature) are the main discrepancies found with our results for water. Our simulations predict that under isothermal conditions K_H is larger in ice than in water while the values derived from DINS data at 269 K forecast that K_H is much lower in ice Ih than in water.

In the face of the discrepancies found between our simulation results for K_H and those derived from neutron-scattering experiments, we have related K_H to other thermodynamic properties pursuing to gain a deeper understanding of the implication of such differences. We find that the maximum in the density of water is not related to any significant effect in the proton kinetic energy at atmospheric pressure. In the analysis of C_p our simulations display reasonable results for both water and ice Ih at 271 K. The K_H contribution to C_p amounts to about 4 J mol^{-1} K^{-1} in water (5% of C_p). However, the temperature dependence of K_H as derived from DINS experiments leads to a dramatic negative contribution to C_p of about -10^4 J mol^{-1} K^{-1}. This value cannot be directly compared to experimental data, but both its sign and magnitude seem to be outside any reasonable physical boundary. At this point it is clear that further independent experiments and theoretical calculations are necessary to clarify this question.

The calculated values of K_O and K_H in water and ice at isothermal conditions show that the largest results are always associated with the solid phase. This fact determines the sign of the isotopic shifts in the melting temperature upon isotopic substitution of either H or O atoms. In both cases the model

predictions are in agreement to experiment. The temperature dependence of K_H in ice Ih has shown satisfactory agreement with results derived from PIMD simulations based on *ab initio* DFT calculations using the SIESTA code.[21,22]

Summarizing, it is clear that an empirical potential model of water cannot reproduce quantitatively all thermodynamic properties of the real system. However, it is the combined analysis of several thermodynamic properties, such as the proton kinetic energy K_H, the intramolecular and intermolecular contributions to K_H, the heat capacity C_p, the isotopic shifts in melting temperatures, and the density-temperature curve of water, that led us to believe that the employed model provides realistic results for the temperature dependence of K_H in water and ice Ih at atmospheric pressure.

*ramirez@icmm.csic.es

[1] C. Andreani, D. Colognesi, E. Degiorgi, and M. A. Ricci, J. Chem. Phys. **115**, 11243 (2001).

[2] G. Reiter and R. Silver, Phys. Rev. Lett. **54**, 1047 (1985).

[3] G. F. Reiter, J. C. Li, J. Mayers, T. Abdul-Redah, and P. Platzman, Braz. J. Phys. **34**, 142 (2004).

[4] C. Pantalei, A. Pietropaolo, R. Senesi, C. Andreani, S. Imberti, J. Mayers, C. Burnham, and G. Reiter, Phys. Rev. Lett. **100**, 177801 (2008).

[5] A. Pietropaolo, R. Senesi, C. Andreani, A. Botti, M. A. Ricci, and F. Bruni, Phys. Rev. Lett. **100**, 127802 (2008).

[6] A. Pietropaolo, R. Senesi, C. Andreani, A. Botti, M. A. Ricci, and F. Bruni, Phys. Rev. Lett. **103**, 069802 (2009).

[7] A. K. Soper, Phys. Rev. Lett. **103**, 069801 (2009).

[8] D. Flammini, M. A. Ricci, and F. Bruni, J. Chem. Phys. **130**, 236101 (2009).

[9] A. Pietropaolo, R. Senesi, C. Andreani, and J. Mayers, Braz. J. Phys. **39**, 318 (2009).

[10] G. Reiter, C. Burnham, D. Homouz, P. M. Platzman, J. Mayers, T. Abdul-Redah, A. P. Moravsky, J. C. Li, C.-K. Loong, and A. I. Kolesnikov, Phys. Rev. Lett. **97**, 247801 (2006).

[11] R. Moreh and D. Nemirovsky, J. Chem. Phys. **133**, 084506 (2010).

[12] C. J. Burnham, G. F. Reiter, J. Mayers, T. Abdul-Redah, H. Reichert, and H. Dosch, Phys. Chem. Chem. Phys. **8**, 3966 (2006).

[13] J. A. Morrone, V. Srinivasan, D. Sebastiani, and R. Car, J. Chem. Phys. **126**, 234504 (2007).

[14] J. A. Morrone and R. Car, Phys. Rev. Lett. **101**, 017801 (2008).

[15] M. F. Herman, E. J. Bruskin, and B. J. Berne, J. Chem. Phys. **76**, 5150 (1982).

[16] M. Parrinello and A. Rahman, J. Chem. Phys. **80**, 860 (1984).

[17] D. N. Timms, A. C. Evans, M. Boninsegni, D. M. Ceperley, J. Mayers, and R. O. Simmons, J. Phys.: Condens. Matter **8**, 6665 (1996).

[18] C. P. Herrero, Phys. Rev. B **65**, 014112 (2001).

[19] S. Habershon, T. E. Markland, and D. E. Manolopoulos, J. Chem. Phys. **131**, 024501 (2009).

[20] R. Ramírez and C. P. Herrero, J. Chem. Phys. **133**, 144511 (2010).

[21] P. Ordejón, E. Artacho, and J. M. Soler, Phys. Rev. B **53**, R10441 (1996).

[22] J. M. Soler, E. Artacho, J. D. Gale, A. García, J. Junquera, P. Ordejón, and D. Sánchez-Portal, J. Phys.: Condens. Matter **14**, 2745 (2002).

[23] R. P. Feynman, *Statistical Mechanics* (Addison-Wesley, New York, 1972).

[24] M. J. Gillan, Philos. Mag. A **58**, 257 (1988).

[25] D. M. Ceperley, Rev. Mod. Phys. **67**, 279 (1995).

[26] C. Chakravarty, Int. Rev. Phys. Chem. **16**, 421 (1997).

[27] G. J. Martyna, A. Hughes, and M. E. Tuckerman, J. Chem. Phys. **110**, 3275 (1999).

[28] M. E. Tuckerman, in *Quantum Simulations of Complex Many–Body Systems: From Theory to Algorithms*, edited by J. Grotendorst, D. Marx, and A. Muramatsu (NIC, FZ Jülich, 2002), p. 269.

[29] M. E. Tuckerman and A. Hughes, in *Classical & Quantum Dynamics in Condensed Phase Simulations*, edited by B. J. Berne and D. F. Coker (Word Scientific, Singapore, 1998), p. 311.

[30] M. E. Tuckerman, B. J. Berne, G. J. Martyna, and M. L. Klein, J. Chem. Phys. **99**, 2796 (1993).

[31] G. J. Martyna, M. E. Tuckerman, D. J. Tobias, and M. L. Klein, Mol. Phys. **87**, 1117 (1996).

[32] P. Pacheco, *Parallel Programming with MPI* (Morgan-Kaufmann, San Francisco, 1997).

[33] R. Moreh, D. Levant, and E. Kunoff, Phys. Rev. B **45**, 742 (1992).

[34] J. P. Perdew, K. Burke, and M. Ernzerhof, Phys. Rev. Lett. **77**, 3865 (1996).

[35] N. Troullier and J. L. Martins, Phys. Rev. B **43**, 1993 (1991).

[36] L. Kleinman and D. M. Bylander, Phys. Rev. Lett. **48**, 1425 (1982).

[37] M. V. Fernández-Serra and E. Artacho, Phys. Rev. Lett. **96**, 016404 (2006).

[38] M. V. Fernández-Serra and E. Artacho, J. Chem. Phys. **121**, 11136 (2004).

[39] J. Wang, G. Román-Pérez, J. M. Soler, E. Artacho, and M.-V. Fernández-Serra, J. Chem. Phys. **134**, 024516 (2011).

[40] C. Andreani, E. Degiorgi, R. Senesi, F. Cilloco, D. Colognesi, J. Mayers, M. Nardone, and E. Pace, J. Chem. Phys. **114**, 387 (2001).

[41] M. F. Chaplin, in *Water of Life: The Unique Properties of H₂O*, edited by R. M. Lynden Bell, S. C. Morris, J. D. Barrow, J. L. Finney, and C. L. Harper Jr. (CRC, Boca Raton, 2010), p. 69.

[42] K. Nygård, M. Hakala, S. Manninen, A. Andrejczuk, M. Itou, Y. Sakurai, L. G. M. Pettersson, and K. Hämäläinen, Phys. Rev. E **74**, 031503 (2006).

[43] C. L. van Panthaleon van Eck, H. Mendel, and J. Fahrenfort, Proc. R. Soc. London, Ser. A **247**, 472 (1958).

[44] C. A. Angell, M. Oguni, and W. J. Sichina, J. Phys. Chem. **86**, 998 (1982).

[45] R. Feistel and W. Wagner, J. Phys. Chem. Ref. Data **35**, 1021 (2006).

[46] G. S. Kell, J. Chem. Eng. Data **20**, 97 (1975).